Analysis of haze disperse composition variation at increase of atmospheric turbidity by AOT measurements in Tomsk

R.F. Rakhimov, D.M. Kabanov, and E.V. Makienko

Institute of Atmospheric Optics,
Siberian Branch of the Russian Academy of Sciences, Tomsk

Received March 14, 2006

Statistically averaged variability of the aerosol component has been studied based on data of spectral measurements of AOT in Tomsk. Characteristic variations of the particle size spectrum of atmospheric hazes occurring at increase of the atmospheric turbidity are analyzed based on inversion of the spectral data. Estimates show that the increase of atmospheric turbidity is stipulated, on the whole, by growing content of accumulation fraction of aerosol. It is characteristic of the atmosphere under conditions of increased turbidity that pronounced medium size particle mode is formed. Analysis of histograms of distribution density $\xi(\tau)$ of the spectral values $\tau(\lambda_i)$ over the interval of the within-year variability (repeatability) performed for years from 2000 until 2002 has shown that, despite a noticeable interannual difference in statistical distribution of AOT values, all histograms in the annual measurement series of the repeatability have a pronounced maximum and a stable interval of the most probable values.

Introduction

The role of different geophysical factors in annual and seasonal variability of the "optical weather" over West Siberia has been analyzed based on the results of ground-based and airborne measurements of atmospheric aerosol parameters.[1] Interannual trend of the columnar aerosol content has been studied, the signs of periodicity of variations have been revealed, which are caused by circulation processes of the sizes exceeding the region under study. We consider the influence of atmospheric processes determining the variability of the aerosol optical characteristics under conditions of air mass change in the region as well as at diurnal variations of meteorological quantities.

Microphysical interpretation of the state of aerosol component of the atmosphere[2,3] has shown that not only seasonal variations of weather-forming factors interlace, in a complicated way, with the diurnal cycles of variations of meteorological quantities, thus making specific regional aerosol "optical weather" of West Siberia, but also with the irregular statistics of forest and peatbog fires.[4]

On the one hand, the results of optical observations[2,3] show that annual variations of the aerosol extinction coefficient in the visible wavelength range (under the effect of random anomalous emissions of aerosol from underlying surface, including the biomass burning) reach, in maximum, 400–600% of the most probable values (MPV). At the same time, according to the estimates,[3] one can say about interannual stability of the MPV of the aerosol extinction coefficient in visible and near IR ranges. Interannual displacements of the maxima of statistical distribution of the values of the aerosol extinction coefficient are 2–7% and do not come out of the range of measurement errors of ± 0.016 km^{-1}.

On the whole, according to literature data,[1–5] regional background of aerosol turbidity of the atmosphere depends not only on the activity of the local sources, but also the efficiency of aerosol and gas anomalies dispersal at long-range transport.

Specific features of the circulation processes over West Siberia are characterized by quite frequent alternation of air masses (AM), Arctic with not only continental but also with the tropical ones coming to the region from vast territories of Kazakhstan and Middle Asia.[6,7] Seasonal peculiarity of the sequences of invasion of different types of AM and their residence time in the region determine the dynamics of variations of the effective height of the mixing layer and some peculiarities in the development of thermal stratification of the troposphere.

Homogeneity of different types of air masses is not absolute, because the underlying surface, over which air masses move, is not uniform. These differences in meteorological parameters are not so noticeable in comparison with the differences between two neighbor AM, but essential gradients of aerosol caused by anomalous emissions of aerosol forming compounds from regional sources are observed even inside one AM. All this is evidence of the necessity of supplementing the conclusions drawn in Refs. 2, 3, and 8 by investigations of the peculiarities of variations of the atmospheric aerosol transmission not only along the near-ground paths but also in the entire atmospheric column.

1. Measured results

The spectral measurement data on the aerosol optical thickness (AOT) obtained in Tomsk in the period since 2000 until 2002 (~1280 spectra) are analyzed in this paper. Measurements of AOT were

0235-6880/06/10 756-09 $02.00

carried out mainly in the periods from spring until fall and provided for hourly mean spectral values. Temporal series of the spectral values of AOT $\tau_{\lambda_i}(k)$ at four wavelengths measured in 2000 are shown in Fig. 1*a*, where k is the number of the realization (numeration of the realizations corresponds to the sequence of measurements).

The used series of observations are characterized by noticeably nonuniform distribution of the data over observations during the experiments. The matter is that the bulk of data, compiled during a day, changed depending on weather conditions and on the synoptic processes being developed in the region (mainly the cloud fraction).

The obtained data show that the episodes of high transparency and unordinary turbidity of the atmosphere have different duration, changing each other many times, are distributed over the period of observations quite irregularly (see Fig. 1*a*). According to Ref. 7, synoptic situation in 2000 in the region of measurements has developed mainly due to competition of two types of air masses: continental (51%) and arctic (37%).

At the same time, quite long periods of enhanced turbidity of the atmosphere were observed for the short-wave range, where the values AOT are determined by contribution of particles of accumulative and intermediate fractions (see, for example, realizations 276 to 360). Numerous forest fires were observed in the region in this period, the consequences of which were vast emissions of smoke aerosol into the atmosphere that caused high values of atmospheric turbidity for visible radiation.

Detailed analysis of the time series of AOT, column density of water vapor W_c, temperature, relative and absolute humidity in the near-ground layer, wind speed and direction D_w shows that the dramatic variations of their values not always coincide with each other in time. They are caused not only by daily breaks in measurements or by the change of air masses, but also by inhomogeneity of the spatial distribution of aerosol fractions (accumulative, intermediate, and coarse) as well as by variations of meteorological parameters both inside an AM and at the boundary between the masses. For example, in some episodes (Fig. 1*b*) in the short-wave range $\tau(\lambda = 0.372\ \mu m)$ one can note quite complicated change of the values of AOT correlated with the column density of water vapor, while no such correlation is observed for $\tau(\lambda = 1.047\ \mu m)$.

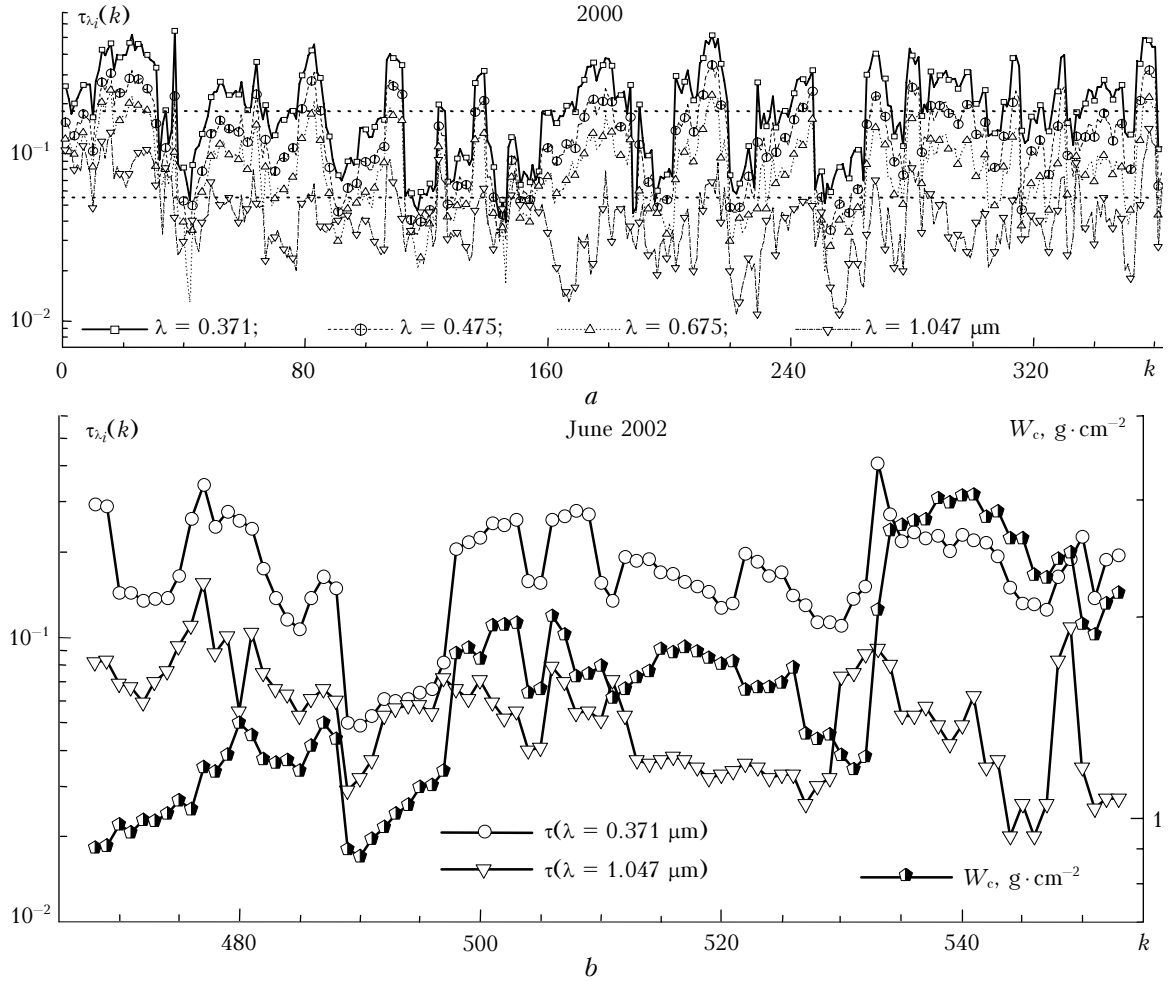

Fig. 1. Time series of AOT (*a*) and water vapor column density W_c (*b*).

The essential, not always correlated change of the spectral values $\tau_{\lambda_i}(k)$ is also seen in the time series (Fig. 1) (see, for example, the dynamics of the AOT values at 1.047 and 0.371 μm). The amplitude of deviation of the AOT from the annual mean value (for example, at $\lambda = 0.371$ μm $\tau_{mean} \sim 0.2$) sometimes reaches 200–250%.

2. Analysis of observations

The three-year mean spectral values of AOT reveal quite smooth dependence (Table 1, 2nd column), which in the considered wavelength range is well approximated by the Angström formula

$$\tau_{mean}(\lambda) = 0.0603\,\lambda^{-1.304}. \qquad (1)$$

Analysis of variability of the spectral values of AOT in the total set of the measured data (since 2000 until 2002, ~ 1280 realizations) shows (Fig. 2) that the distribution of the frequency of occurrence $\xi(\tau_\lambda)$ exhibits three characteristic intervals in the realizations of the measured values $\tau(\lambda_i)$. In particular, in the data at the wavelength $\lambda_i = 0.438$ μm one can isolate these intervals as $[\tau < 0.07]$, $[0.07 < \tau < 0.3]$, and $[\tau > 0.3]$.

One should note that in the range of MPV from the interval $[0.07 < \tau < 0.3]$ the distribution of the frequency of occurrence $\xi(\tau_\lambda)$ well follows the lognormal law

$$\xi(\tau) = \frac{\xi_{0\lambda}}{\sqrt{2\pi}\,\tau \ln\sigma_\lambda} \exp\left\{-\frac{\ln^2(\tau/\tau^{\lambda}_{MPV})}{2\ln^2\sigma_\lambda}\right\}, \qquad (2)$$

practically at all wavelengths. Here $\xi_{0\lambda}$, σ_λ, and τ^{λ}_{MPV} are the parameters of the distribution at different wavelengths.

Table 1

λ, μm	τ_{mean}	rmsd	τ_{MPV}	Δ	τ^{north}_{mean}	τ^{south}_{mean}	τ^{north}_{MPV}	τ^{south}_{MPV}	Δ_{north}	Δ_{south}
1	2	3	4	5	6	7	8	9	10	11
0.371	0.227	0.167	0.134	0.402	0.154	0.267	0.135	0.139	0.130	0.628
0.408	0.198	0.142	0.122	0.539	0.134	0.231	0.129	0.126	0.039	0.587
0.438	0.175	0.126	0.113	0.539	0.119	0.204	0.105	0.120	0.126	0.523
0.475	0.158	0.113	0.102	0.482	0.106	0.184	0.096	0.105	0.098	0.547
0.500	0.148	0.106	0.093	0.454	0.100	0.173	0.089	0.098	0.117	0.549
0.547	0.130	0.093	0.082	0.561	0.086	0.153	0.078	0.091	0.099	0.510
0.675	0.096	0.066	0.059	0.520	0.064	0.112	0.063	0.061	0.030	0.584
0.871	0.070	0.048	0.041	0.487	0.045	0.083	0.038	0.044	0.185	0.607
1.047	0.060	0.041	0.036	0.510	0.042	0.068	0.033	0.035	0.235	0.643

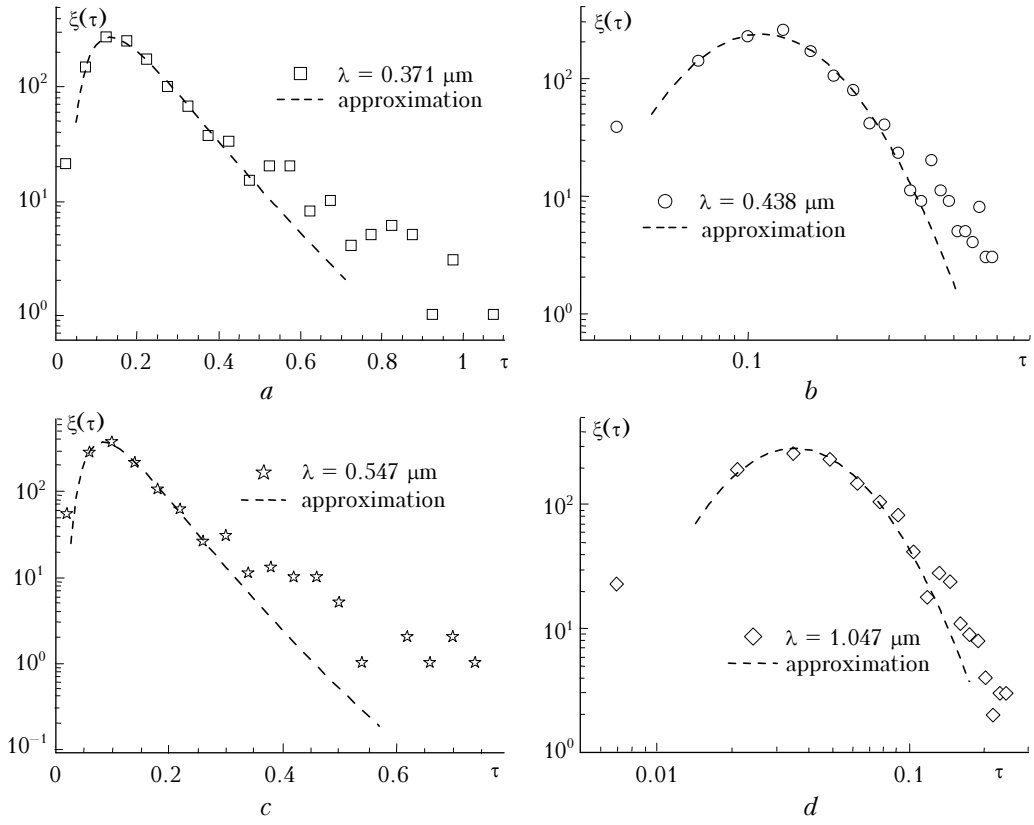

Fig. 2. Distribution of the frequency of occurrence of the AOT values.

At the same time, quite wide (if estimated on linear scale) interval $\tau(\lambda = 0.438\ \mu m) > 0.3$ (Fig. 2*b*) lies out of the aforementioned regularity of the statistical distribution of AOT. Here the histograms of the $\xi(\tau_\lambda)$ distribution constructed from annual ensembles of realizations of the spectral values of AOT do not obey the lognormal law, having noticeably different shapes not only in different years, but also at different wavelengths.

The frequency of occurrence of $\tau(\lambda_i)$ values for very transparent situations, for example, at $\tau(0.438\ \mu m) < 0.07$ also contradicts the aforementioned regularity (2) (Figs. 2*b* and *d*). The fraction of such atmospheric situations occurring in the region under study, among the total statistics of the observations, is essential and densely occupies certain interval of variations.

Statistics of atmospheric situations with small AOT values $\tau(\lambda_i) < 0.07$ also is not stable and changes from year to year (Fig. 3). Annual frequency of occurrence of such situations depends on specific features of the synoptic processes and, in particular, on the frequency of invasion (to the region of measurements) of arctic AM, the content of accumulative fraction in which is noticeably lower than in mid-latitude AM.[7–9] Significant remoteness of the main region of formation of arctic AM from continental sources of aerosol forming compounds predetermines the deficiency of fine aerosol fraction (as compared with other types of AM) mentioned in Refs. 7 and 10.

Comparison of the normalized values of the distribution of the frequency of occurrence of AOT $\xi(\tau)/\xi_0$ constructed using some (within-year) ensembles of realizations at $\lambda = 0.371\ \mu m$ is shown in Fig. 3, which shows that not only quite well coinciding statistics of their variations is observed in the vicinity of MPV but also the interannual stability of the most probable (during a year) spectral values of the $\tau_{MPV}(\lambda_i)$.

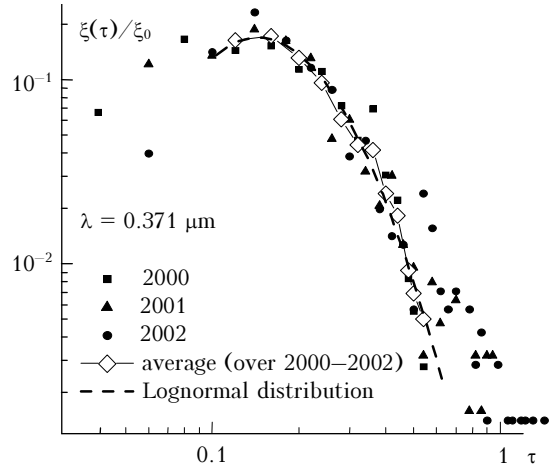

Fig. 3. Normalized values of the frequency of occurrence $\xi(\tau)/\xi_0$.

Analogous regularity was revealed eralier[3] from the measured results on the aerosol extinction coefficient along near-ground paths β_ε [km^{-1}]. Comparison of the distribution of the frequency of occurrence of different values of AOT with analogous data on β_ε showed[3] that the higher percentage of situations with high transmission is characteristic of $\xi(\tau)$ than of $\xi(\beta_\varepsilon)$.

Differences in the statistical distribution of two optical parameters in transparent atmospheric situation are, obviously, caused by longer time of filling the atmospheric column in arctic AM by accumulative aerosol fraction.[2,9,12] Cooling of the underlying surface which occurs at invasion of arctic AM to the region damps the convective fluxes. In this case, only the aerosol content in the near-ground layer noticeably changes under the effect of local sources, but not in the atmospheric column. This is the cause of qualitative differences in $\xi(\tau)$ and $\xi(\beta_\varepsilon)$ in the shortwave range.

From comparison of the most probable $\tau_{MPV}(\lambda_i)$ values with near-ground $\beta_{\varepsilon,MPV}(\lambda_i)$ one can conclude that the height of the "effective" filling of the atmosphere with aerosol varies from 0.8 to 1.3 km that agrees with the estimates[8] obtained from "mean" spectral data on the aforementioned parameters.

The width of the lognormal distribution $\xi(\tau_\lambda)$, following the parameters of the approximation (2), in the range of MPV shows a weak tendency to narrowing with increasing wavelength.

The spectral values $\tau_{MPV}(\lambda_i)$ estimated by Eq. (2) are shown in the 4th column of Table 1. One should note that the differences in the mean spectral dependence $\tau_{mean}(\lambda_i)$ (2nd column) from the most probable values $\tau_{MPV}(\lambda_i)$ sometimes reach ~50% (see the 5th column, where $\Delta(\lambda_i) = (\tau_{mean} - \tau_{MPV})/(\tau_{mean} + \tau_{MPV})$). The estimates of the variance of the obtained data are shown in the 3d column.

Analysis of diurnal variations of AOT in warm season shows[9] that the essential factor of the change of the aerosol content in the lower layer of the troposphere is the near-noon increase of the convective heat flux from the underlying surface. This peculiarity is quite well seen in analyzing the statistical distribution of the AOT values measured in different types of AM.

The data selected for the analysis were obtained in situations close to the most probable values of the atmospheric thickness, i.e., the values, the statistics of which at different wavelengths obeys the lognormal law (2). Actually, the situations $\tau_k(\lambda_i)$ were excluded, for which the values $\tau(\lambda = 0.438\ \mu m)$ exceed 0.45.

Then this data set was divided into two disjoint subarrays. The spectral data, $\tau_k(\lambda_i)$, measured in situations when the near-ground wind direction D_w was mainly from "north" sector, i.e., $270° < D_w < 90°$ were collected in one subarray. The spectral data, $\tau_k(\lambda_i)$, measured mainly in mid-latitude AM with near-ground wind direction from "south" sector, i.e., at $270° > D_w > 90°$ were collected in the second subarray.

Plots of the frequency of occurrence of the AOT values at the boundary wavelengths of the spectral range analyzed obtained using the two selected ensembles of realizations are shown in Fig. 4.

Analogous regularity of transformation of the statistics of AOT values is also observed at other (intermediate) wavelengths.

It is important to note that the estimates of the most probable values $\tau_{MPV}(\lambda)$ for the aforementioned ensembles (they are shown in Table 1, in the 8th and 9th columns) show the spectral dependences slightly different from each other.

As the analysis of the frequency of occurrence of the AOT spectral values shows, the realizations in the ensemble of the "north" have lower percentage of turbid states. The mean statistical values at some wavelength reach the most probable values. Differences between the mean spectral values and the most probable values are only ~10–15% (see the 6th, 8th, and 10th columns of Table 1).

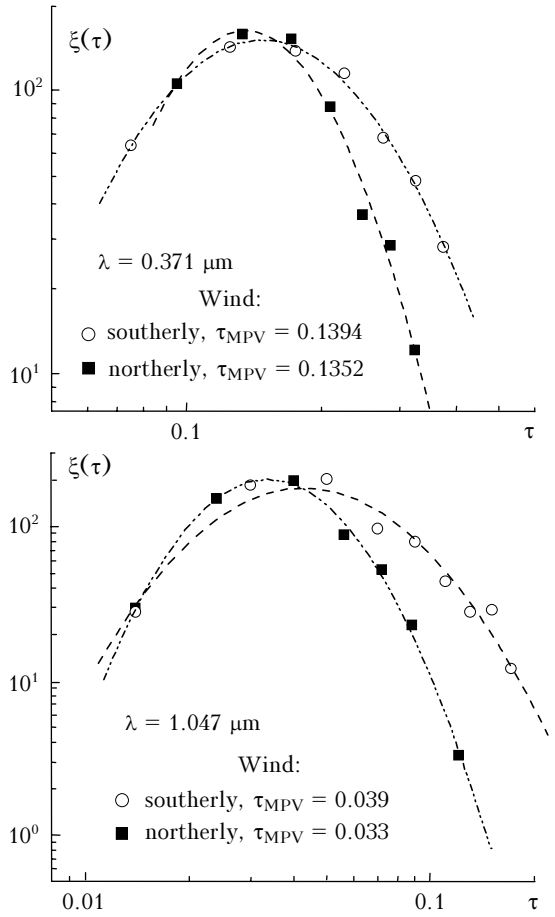

Fig. 4. Distribution of the frequency of occurrence of the AOT values.

Another situation is observed in the ensemble of realizations of the "south" direction of the near-ground wind. In this case the differences between the mean AOT values and the most probable values increase up to 51–64% (see the 7th, 9th, and 11th columns of Table 1). It is seen from the data shown in Fig. 4 that the right-hand branch of the lognormal distribution at southerly winds is noticeably wider both in the shortwave range and in the near IR range. The right-hand boundary of the discussed range of the AOT values exceeds by 100% and more the most probable values $\tau_{MPV}(\lambda_i)$.

The change of the fraction of the enhanced values in the statistics of AOT realizations in the case of "south" AM is seen as a regularity at all wavelengths and occurs in quite a wide range of variations. The estimates of the optical efficiency of particles of different size[12] show that the aforementioned changes in the statistics of realizations of the spectral AOT values cannot be provided by variations of only aerosol fraction. Such changes can be provided by the change of the disperse composition in quite a wide size range, that can take place at intensifying the convective fluxes from the surface.

The hypothesis about the effect of the longer and intense emission of aerosol compounds over heated areas of the underlying surface of southern regions indirectly agrees with other variants of selection of the data of optical measurements.

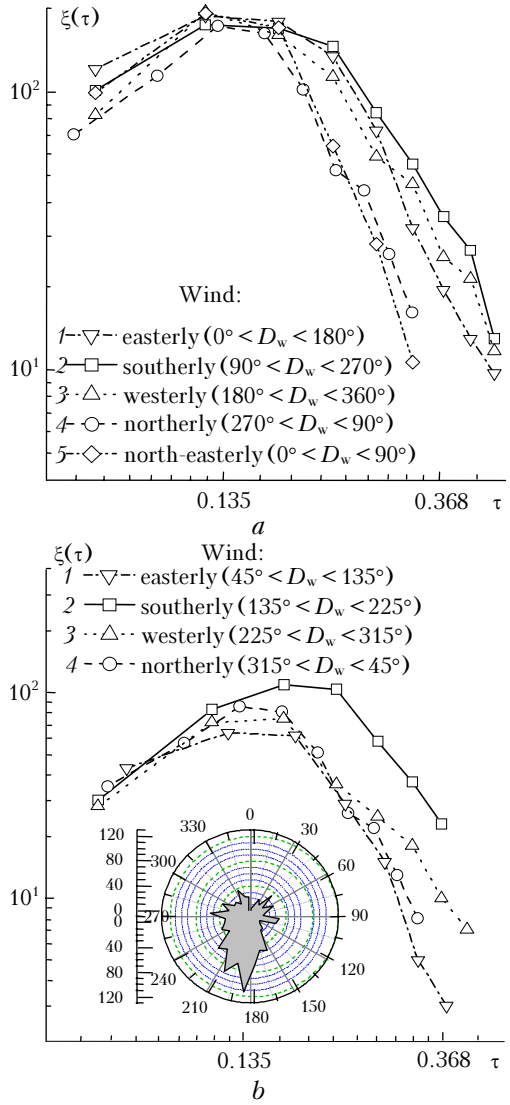

Fig. 5. Distribution of the frequency of occurrence of the AOT values in the range of MPV: $\lambda = 0.438$ μm (*a*), $\lambda = 0.371$ μm (*b*), at division of the measurement data in four disjoint statistical subarrays of realizations $\tau_k(\lambda_i)$.

For example, the attempt of dividing the entire set of realizations of the spectral AOT values into two ensembles with westerly and easterly wind directions has shown that no essential differences in statistics of realizations of the AOT values at such division of the data from that for "southern" one are observed (see curves *1–3*, Fig. 5*a*). The matter is that, in selecting the data in this way, realizations $\tau_k(\lambda_i)$ earlier determining the composition of "south" are now partially in statistical ensembles of "west" and "east" subarrays. At the same time, any method of dividing the ensemble of "north" does not cause essential changes in statistics of $\xi(\tau)$ (see curves *4* and *5*, Fig. 5*a*).

A peculiar situation is observed, if dividing the entire data set according to the wind direction in four disjoint statistical subarrays (Fig. 5*b*).

The initial set of data measured during three years was divided into four ensembles of realizations $\tau_k(\lambda_i)$. The ensemble of realizations $\tau_k(\lambda_i)$ measured, respectively, at the wind direction in the near-ground layer D_w in the range 45–135° was conditionally marked as mainly "east". Similarly, the ensembles of realizations were selected: "south" with $135° < D_w < 225°$, "west" with $225° < D_w < 315°$ and "north" with $315° < D_w < 45°$.

As is easily seen from Fig. 5*b*, the first, third, and fourth ensembles (curves *1*, *3*, and *4* in Fig. 5*b*) have similar and coinciding statistics of the distribution of $\xi(\tau(0.371\ \mu m))$ in the range of MPV, but the ensemble of south direction (curve *2*) is obviously out of this dataset by the characteristics analyzed. The general statistics of wind direction is also shown in Fig. 5.

3. The most probable aerosol disperse composition (model estimates)

The fact that statistics of $\xi(\tau)$ distribution stably obeys the lognormal law (2), as well as the interannual stability of the spectral dependence $\tau_{MPV}(\lambda)$ noted above, have determined the interest in analyzing possible reasons for the observed regularity. This issue has already been discussed in general in Ref. 3, so in this paper the earlier proposed hypotheses have been supplemented with the following analysis of the results obtained.

In particular, the parameters of the distribution (2): $\xi_0(\lambda_i)$, $\tau_{MPV}(\lambda_i)$, $\sigma(\lambda_i)$ were calculated for each wavelength in the range $\lambda_i = 0.37–4.0\ \mu m$ of the ensemble of spectral values of AOT measured in 2000–2002, which are among the most probable states.

Spectral behavior of the values $\tau_{MPV}(\lambda_i)$, which is the result of averaging of many realizations $\tau_k(\lambda_i)$ in the vicinity of the most probable values, has smoothed dependence on the wavelength (curve *1* in Fig. 6*a*). The aerosol size spectrum corresponding to such a spectral dependence is shown in Fig. 6*b*. The spectrum was reconstructed based on solution of the inverse problem (curve *1*) and indicates the sufficiently essential optical contribution of particles of the accumulative fraction (< 0.35 μm).

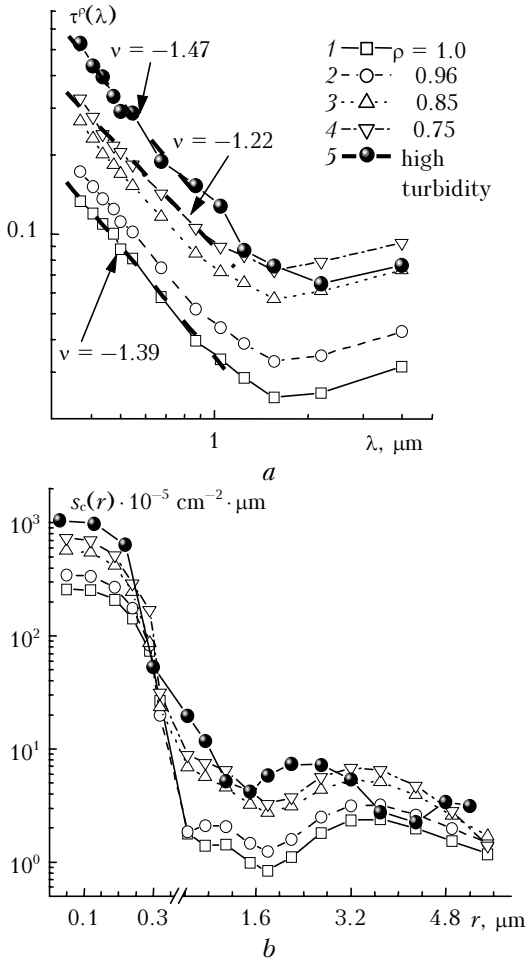

Fig. 6. Variations of the aerosol disperse composition in the range of the most probable states.

Having known the parameters $\xi_0(\lambda_i)$, $\tau_{MPV}(\lambda_i)$, and $\sigma(\lambda_i)$ in Eq. (2) one can estimate spectral variations of the AOT values not only for the most probable states of the aerosol component in the atmosphere, but also in some vicinity of the most probable states, where the regularity of the lognormal distribution $\xi(\lambda_i)$ has been observed. For example, one can try to study the changes in the mean statistics of the disperse composition of haze at its subsequent transition to less probable but quite often observed state with the spectral values $\tau^\rho(\lambda_i)$.

The value $\tau^\rho(\lambda_i)$ was estimated based on the condition (3) using the same value $\rho = \xi/\xi_0 < 1$ for different wavelengths set in advance, as well as the parameters $\xi_0(\lambda_i)$, $\tau_{MPV}(\lambda_i)$, $\sigma(\lambda_i)$:

$$\rho = \frac{\xi[\tau^\rho(\lambda)]}{\xi_{0\lambda}} = \frac{1}{\sqrt{2\pi}\,\tau^\rho \ln\sigma_\lambda} \times$$

$$\times \exp\left\{-\frac{\ln^2(\tau^\rho / \tau_{MPV})}{2\ln^2\sigma_\lambda}\right\} = \text{const}. \qquad (3)$$

Four spectral dependences $\tau^\rho(\lambda_i)$ (curves *1–4*) are shown in Fig. 6*a*, as well as the averaged realizations for only turbid states, which are out of

the range of the most probable states (curve *5*). It is seen that the Angström exponent ν for the short-wave range gradually decreases with the increasing turbidity, according to statistics (2), from 1.39 to 1.22. At the same time, the more steep spectral behavior $\tau(\lambda_i)$ with the Angström exponent of $\nu = 1.47$ is characteristic of situations which are out of the statistics of the most probable states, that is evidence of the noticeable increase of the optical effect of the accumulative fraction.

One should recognize that some mixing of the optical states of the atmosphere occurs in using this way for estimation of the spectral dependence. However, the used approach makes it possible to follow the mean atmospheric change of the optical-microphysical properties of haze at transition from the relatively transparent states of the atmosphere to a more turbid one. In particular, the data on changes in the mean statistics of the contents of different fractions in the disperse composition of the aerosol component of the atmosphere (curves *1–5* in Fig. 6*b*) were obtained from the results of inverting the spectral dependences $\tau^p(\lambda_i)$ (see Fig. 6*a*).

The results of inversion show that, as the probability of observation of the spectral values $\tau^p(\lambda_i)$ increases, the relative content of accumulative and intermediate aerosol fractions decreases, i.e., the less probable states of enhanced turbidity of the atmosphere, as a rule, are caused by enhanced content of the fine aerosol fraction.

The parallel displacement of the curves is observed in the size range of coarse fraction ($r > 1.0$ μm), which can be interpreted as the change of the effective height at which the aerosol ascends from the underlying surface (the height of the mixing layer) at the increasing atmospheric turbidity.

The reason of instability of the annual mean spectral values $\tau_{mean}(\lambda)$ in the range of enhanced turbidity of the atmosphere is not so unambiguous as in the range of small τ, and can be caused by the effect of several geographic factors.[1,9–11] However, essential effect of irregular variations of the content of submicron aerosol particles is also seen in this case.[9,13] Particles of accumulative and intermediate fractions in the atmospheric column are easily transferred to significant distances from sources and have long lifetime.

Measurements show that statistics of the AOT values recorded in the third interval irregularly varied from year to year. The enhanced AOT values are quite often observed in the episodes when AM enriched with smokes of regional forest fires have crossed the measurement path.[9] The large-scale forest and peatbog fires in boreal climatic zone during dry summer season occurs quite frequently. Analysis of spaceborne monitoring of the territory of Tomsk region shows[14,15] that the number of forest fires noticeably varies during 1998–2004 in the range from 100 to 600 events. Obviously, the efficiency of the effect of smoke emissions on statistics of realizations of the enhanced AOT values depends not only on the power and residence time of the products of burning in the atmosphere over the region, but also on the specific features of the synoptic processes in boreal climatic zone,[3,4,7,14–16] that is why their changes are so irregular from year to year. Noticeable interannual variations of annual mean spectral values of AOT occur against the background of interannual stability of the most probable values.

Besides, essential prevalence of statistics of realizations of the most probable AOT values over the range of enhanced values shows that the observed statistics of anomalous aerosol emissions and their power in the region are such that their dispersal in the atmosphere does not essentially affect the most probable level of turbidity of the atmospheric column.

One should consider the analyzed peculiarities of variations of the disperse composition of the atmospheric haze not only as consequences of the relaxation process of aerosol anomalies inside an AM, but also as the near vicinity of the most probable states of the disperse composition of the haze formed due to peculiar features of the circulation processes that determine the alternations of the Arctic AM with continental mid-latitude one that happen quite often.

The dynamics of integral parameters of the disperse structure of the haze is shown in Fig. 7: total cross section S_t and volume V_t of aerosol particles as well as their components — accumulative S_a and V_a and coarse S_c and V_c fractions.

To analyze the changes of microstructure of the haze that may cause that essential variations in AOT in the region of observations, the entire array of measured data was divided into three sub-arrays. Then these sub-arrays representing the mean statistical properties of the aerosol component of the atmosphere were defined as situations of high transmission, moderate, and heavy turbidity. The boundaries of the sub-arrays presented in Fig. 1*a* are shown by dotted lines and have been selected to be approximately of equal lengths, in the scale of variations of $\ln(\tau(\lambda = 0.485\ \mu m))$.

The mean spectral values $\tau_{mean}(\lambda)$ were calculated for the aforementioned ensembles and are shown in Fig. 8*a*. As is seen, the slope of spectral curves essentially changes as the atmospheric thickness increases, ν varies in the range from 0.92 to 1.62.

The results of inversion of the spectral dependences are presented in Fig. 8*b*. They show that the most optically significant changes of the aerosol disperse structure at increasing atmospheric turbidity occur in the range of aerosol particles radii from 0.08 to 0.9 μm. The dynamics of the change of the total cross section and volume of atmospheric particles in different size ranges as the turbidity of the atmospheric column increases is shown in Table 2.

The estimates show more than fivefold increase of the total cross section and volume of particles of accumulative fraction (see Table 2). The effective particle size r_{eff} decreases from ~ 0.2 to 0.14 μm, that confirms the main tendency toward increasing the fraction of the finest optically significant particles.

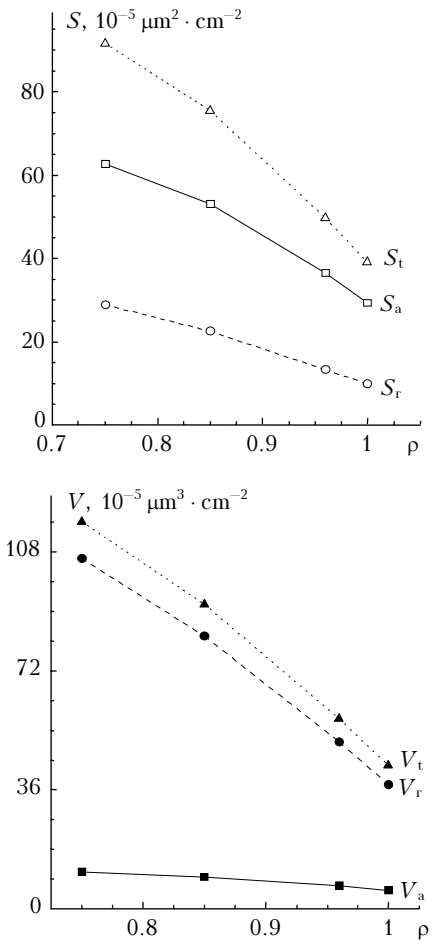

Fig. 7. Dependence of the integral parameters of the disperse structure of haze at increase of the atmospheric turbidity.

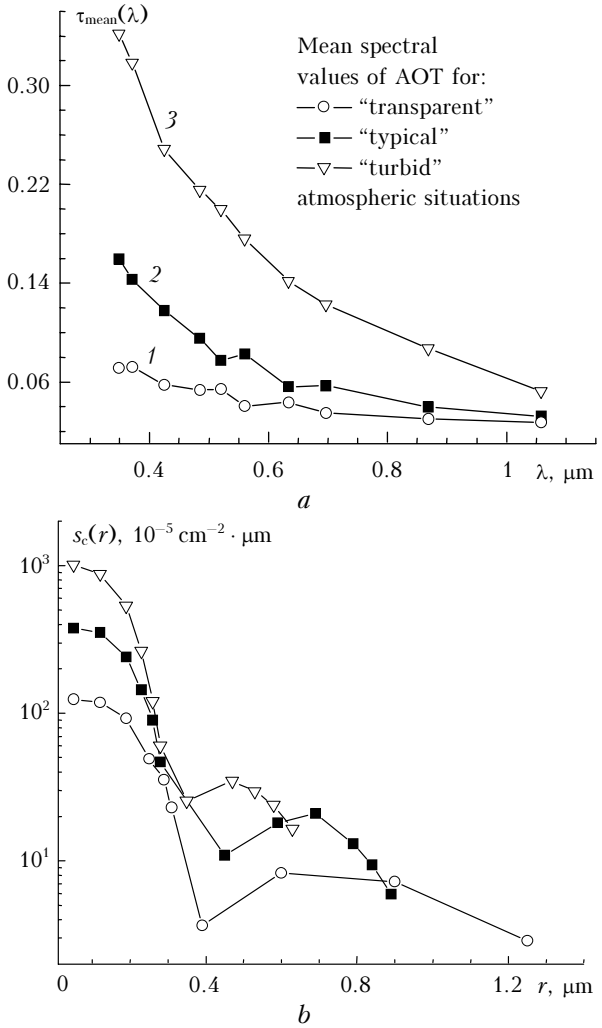

Fig. 8. Spectral change of AOT for three ranges of variations (*a*) and the size spectra reconstructed from them (*b*).

The volume content of larger aerosol fraction does not vary that significant (in comparison with the accumulative fraction).

By inverting the spectral dependences of AOT shown in Fig. 8*a*, we have managed to estimate the spectral variations of the optical contribution of large particles (Fig. 9) as turbidity of the atmospheric column increases, where the tendency toward decrease of the mean radius of particles of intermediate size range r_{eff} from 0.85 to 0.5 μm is observed.

The increase (as the atmospheric turbidity increases) of the optical effect of finer particles of intermediate size range is an evidence of that they came from the size range of accumulative fraction (due to coagulation growth of particles), that is usually observed at dramatic increase of the number density of the latter, for example, at enrichment of an AM with smoke aerosols over the places of large-scale forest fires.[3]

Table 2. Change of the total cross section S_t and volume V_t of aerosol particles and their fractions in different size ranges as the turbidity of the atmospheric column increases

Integral parameter	Atmospheric column		
	Transparent	Mean turbidity	Heavy turbidity
S_t 10^{-5} μm² · cm^{-2}	33.0	81.0	176.0
S_a 10^{-5} μm² · cm^{-2}	26.0	68.0	168.0
S_r 10^{-5} μm² · cm^{-2}	7.0	13.0	8.0
V_t 10^{-5} μm³ · cm^{-2}	10.4	18.5	29.5
V_a 10^{-5} μm³ · cm^{-2}	4.90	11.5	25.2
V_r 10^{-5} μm³ · cm^{-2}	5.5	7.0	4.5

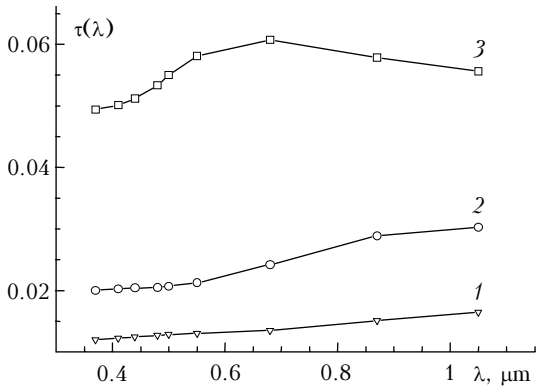

Fig. 9. Transformation of the spectral dependence of the optical contribution of intermediate size fraction of aerosol as atmospheric turbidity increases. Curve numbers correspond to notations in Fig. 8*a*.

Conclusions

Analysis of statistical variability of AOT measured in the period since 2000 until 2002 shows that three characteristic intervals of realization of the measured values $\tau_k(\lambda_i)$ are seen in the distribution of the frequency of occurrence of the AOT values at different wavelengths $\xi(\tau(\lambda_i))$.

The distribution of the frequency of occurrence $\xi(\tau)$ in the range of the most probable values well follows the lognormal law. The width of the model approximation (2) of the distribution $\xi(\tau(\lambda))$ has the tendency toward narrowing with increasing wavelength. Only very transparent situations are noticeably out of the aforementioned statistical regularity, for example, for $\tau(\lambda = 0.438\ \mu m) < 0.08$, as well as with anomalously high values $\tau(0.438\ \mu m) > 0.4$.

In spite of the fact that circulation processes formed different (for different years) weather conditions of optical observations in Tomsk (noticeable scatter of the data according to synoptic criteria[4]), analysis of the frequency of occurrence of the spectral values of AOT $\xi(\tau)$ shows quite good interannual stability of their most probable values $\tau_{MPV}(\lambda_i)$.

Air masses with enhanced turbidity of the atmospheric column contain, as a rule, the well pronounced mode of intermediate size aerosol particles. The estimates show more than fivefold increase of the total cross section and volume of particles of accumulative fractions. The effective particles size r_{eff} decreases from ~ 0.2 to 0.14 μm. The volume content of larger aerosol fractions does not undergo that significant change.

The main factor of the change of transmission of the atmosphere in the wavelength range $\lambda < 0.75$ μm is the change of the optical contribution of accumulative fraction.

Acknowledgments

Authors would like to thank S.M. Sakerin for constructive discussion of the presented results and useful remarks.

References

1. M.V. Panchenko, Yu.A. Pkhalagov, R.F. Rakhimov, S.M. Sakerin, and B.D. Belan, Atmos. Oceanic Opt. **12**, No. 10, 883–894 (1999).
2. R.F. Rakhimov, V.N. Uzhegov, E.V. Makienko, and Yu.A. Pkhalagov, Atmos. Oceanic Opt. **17**, Nos. 5–6, 339–357 (2004).
3. R.F. Rakhimov, V.N. Uzhegov, E.V. Makienko, and Yu.A. Pkhalagov, Atmos. Oceanic Opt. **18**, No. 7, 506–513 (2005).
4. E.V. Makienko, R.F. Rakhimov, S.M. Sakerin, D.M. Kabanov, and V.N. Uzhegov, in: *Proc. of the 5th Int. Conf. on Wildlife Fires: Initiation, Spread, Suppressing and Ecological Consequences* (Krasnoyarsk, 2003), pp. 285–287.
5. K.Ya. Kondratyev, Atmos. Oceanic Opt. **15**, No. 4, 267–284 (2002).
6. V.I. Vorob'ev, *Synoptic Meteorology* (Gidrometeoizdat, Leningrad, 1991), 616 pp.
7. B.D. Belan, T.M. Rasskazchikova, and T.K. Sklyadneva, Atmos. Oceanic Opt. **18**, No. 10, 796–801 (2005).
8. V.N. Uzhegov, Yu.A. Pkhalagov, D.M. Kabanov, S.M. Sakerin, and M.V. Panchenko, Atmos. Oceanic Opt. **18**, Nos. 5–6, 367–372 (2005).
9. E.V. Makienko, R.F. Rakhimov, S.M. Sakerin, and D.M. Kabanov, Atmos. Oceanic Opt. **15**, No. 7, 531–540 (2002).
10. S.M. Sakerin, R.F. Rakhimov, E.V. Makienko, and D.M. Kabanov, Atmos. Oceanic Opt. **13**, No. 9, 754–758 (2000).
11. R.F. Rakhimov, S.M. Sakerin, E.V. Makienko, and D.M. Kabanov, Atmos. Oceanic Opt. **13**, No. 9, 759–765 (2000).
12. G.M. Krekov and R.F. Rakhimov, *Optical Radar Model of Continental Aerosol* (Nauka, Novosibirsk, 1982), 200 pp.
13. E.V. Makienko, R.F. Rakhimov, V.N. Uzhegov, and Yu.A. Pkhalagov, Atmos. Oceanic Opt. **16**, No. 12, 1008–1012 (2003).
14. S.V. Afonin, V.V. Belov, and Yu.V. Gridnev, Atmos. Oceanic Opt. **13**, No. 11, 921–929 (2000).
15. S.V. Afonin and V.V. Belov, Atmos. Oceanic Opt. **14**, No. 8, 634–638 (2001).
16. V.E. Zuev, B.D. Belan, and G.O. Zadde, *Optical Weather* (Nauka, Novosibirsk, 1990), 192 pp.